

---

---

**Visible-Blind Au/ZnO Colloidal Quantum Dots (CQDs) Based  
Spectrum Selective Schottky Photodiodes on Silicon Substrates\***

---

---

Contents

2.1	Introduction.....	35
2.2	Experimental Details.....	36
2.2.1	Preparation of colloidal ZnO QDs.....	36
2.2.2	Fabrication of Photodetector .....	37
2.3	Result and Discussion.....	40
2.3.1	Structural Characterization of as-grown ZnO QD.....	40
2.3.2	Electro-Optical Characterization .....	43
2.3.2.1	Current Voltage Characterization .....	43
2.3.2.2	Capacitance Voltage characteristics.....	45
2.3.2.3	Responsivity Characterization .....	46
2.3.2.4	Time response analysis .....	52
2.4	Conclusion .....	53

\*Part of this work has been published as:

Yogesh Kumar et al. "Visible-blind Au/ZnO Quantum dots Based Highly Sensitive and Spectrum Selective Schottky Photodiode," *IEEE Transactions on Electron Devices*, vol. 64, no. 7, pp. 2874-2880, 2017.



---

## Visible-Blind Au/ZnO Colloidal Quantum Dots (CQDs) Based Spectrum Selective Schottky Photodiodes on Silicon Substrates

---

### 2.1 Introduction

The spectrum selective photodetectors with full width at half maximum (FWHM) of  $\Delta\lambda$  (which should be less than 100 nm (Jansen-van Vuuren *et al.*, 2016)) at any wavelength  $\lambda$  are used to detect light with effective wavelengths in the range of  $\lambda-\Delta\lambda$  and  $\lambda+\Delta\lambda$ . As discussed in Chapter 1, the spectrum selective ultraviolet (UV) photodetectors with high detectivity, high signal-to-noise ratio and fast response speed are important devices for multiple applications including UV-photolithography, flame sensing, water sterilization, medical and biological etc. (Monroy *et al.*, 2001) and (Aufiero *et al.*, 2006). It is already discussed in Chapter-1 that transition metal oxide nanostructures specially solution processed colloidal ZnO QDs can be explored for UV detectors due to the large direct band gap energy  $\sim 3.37$  eV (D. Y. Guo *et al.*, 2014), high thermal and chemical stabilities (Ali and Chakrabarti, 2010), and (Yadav *et al.*, 2014) low-cost low-temperature solution processing based fabrication method (Wang, 2004), flexibility of using different substrates (Wang, 2004; Krivchenko *et al.*, 2008; Ick Son *et al.*, 2013) for device fabrication and size-dependent band gap energy of the ZnO QDs.

In this chapter, we have fabricated Au/ZnO QDs based Schottky diode photodetector on n-Si substrate using low-cost solution process technique. The ZnO QD based Schottky diode photodetector shows the narrowband spectral response and remains visibly blind. The photodiode also shows very high responsivity compared to

other reported Schottky photodiodes (Yadav *et al.*, 2015). The Schottky photodiode is also analyzed for transient response under the UV illumination. The outline of this chapter can be given as follows:

Section 2.2 presents the experimental details of the synthesis of ZnO QDs and the fabrication procedure of the Schottky photodiode on silicon substrate. Section 2.3 includes the results and discussion of the film morphology of ZnO QDs and electro-optical characteristics of the photodiode such as current-voltage, photo responsivity and time response under dark and UV illumination of the PD.

## 2.2 Experimental Details

### 2.2.1 Preparation of colloidal ZnO QDs

For the preparation of ZnO QDs, the precursor Zinc-acetate dihydrate (500 mM) was dissolved in 2-methoxyethanol (coordinating ligand) and continuously stirred under the steady flow of nitrogen. The temperature was gradually raised up to 60 °C and then equivalent molar ratio of MEA (reagent) was injected quickly enough to lead a short nucleation with slower growth of particles (Murray *et al.*, 2001). The temperature of the coordinating ligand was maintained at 60 °C so that the reagent is decomposed completely to enhance the growth of the ZnO QDs. To ensure the minimal particle size, the heating of the solution was immediately stopped to bring it to the room temperature so that the growth of the particles after the discrete nucleation could remain in the limits of Bohr's radius (~2.87 nm for ZnO). The solution was then further stirred for 24 hrs under nitrogen environment and then filtered using PVDF membrane (0.22 μm) to filter out the unreacted particles from the solution. The Figure 2. 1 shows the detailed flow chart of the ZnO QDs synthesis process.

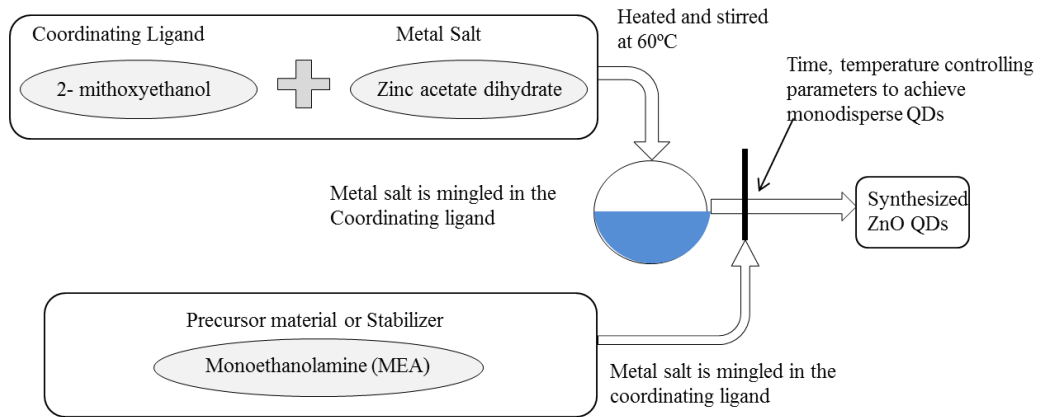


**Figure 2. 1:** Synthesis flow chart of ZnO QDs under the inert environment.



**Figure 2. 2:** Spin coater setup for thin film deposition.

### 2.2.2 Fabrication of Photodetector

For the fabrication of the thin film devices, heavily doped silicon (n-Si) substrates are cleaned ultrasonically using trichloroethylene, acetone, and de-ionized water (DI) (resitivity-18 M $\Omega$  Millipore-USA) sequentially. Then the substrate was dipped in the solution of the H<sub>2</sub>SO<sub>4</sub> : H<sub>2</sub>O<sub>2</sub> (2:3) for 10 min. to removes the metallic particles from the surface of the substrate. Further, the substrate is frequently rinsed under the running DI

water to remove the acidic contents. The substrate was submerged in the solution of HF: DI (1:10) for 2 min. to remove the unwanted native oxides grown over the surface of the substrate. Afterward, the wafer was rinsed under the running DI water for two times and then dried in prebaked oven for 15 min. at 90 °C. Finally, the cleaned and dried substrates were placed for O<sub>2</sub> plasma cleaning (Cute, Femto Science) for 5 min. The cleaned n-Si (111) substrates (moderately doped with surface resistivity ~2-7 ohm/cm<sup>2</sup>) are placed on the spin-coater (SPM-150LC TSE-system GmbH, Germany) as shown in Figure 2. 2, and the solution of colloidal ZnO QDs was spin coated with a speed of 3000 rpm for 20 secs. After spin coating, the substrate was immediately placed on the prebaked hot plate at 150 °C for 15 min. This process was repeated multiple times to achieve the desired thickness of ~200 nm. The thickness of ZnO film were measured by Reflectometer (F-20 Thin Film UV Analyzer, Filmetrics as shown in Figure 2. 3). Further, the ZnO QDs were annealed for 30 min. at 450 °C under the ambient environment. The Au electrodes as shown in Figure 2. 4 (a) were thermally evaporated on the thin film of ZnO QDs under a vacuum using shadow mask technique. The schematic device structure and the fabricated Schottky photodiode on Si are shown in Figure 2. 4 (a) and (b) respectively. The complete fabrication flow of process as shown in Figure 2. 5.

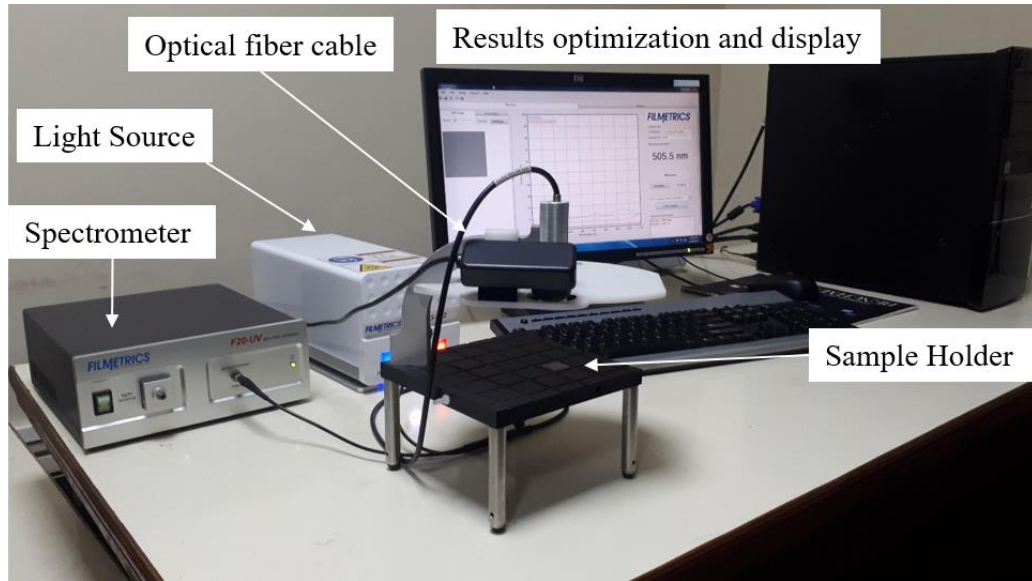


**Figure 2.3:** Experimental setup for optical characterization of thin films (Reflectance and Transmittance) and thickness measurement.

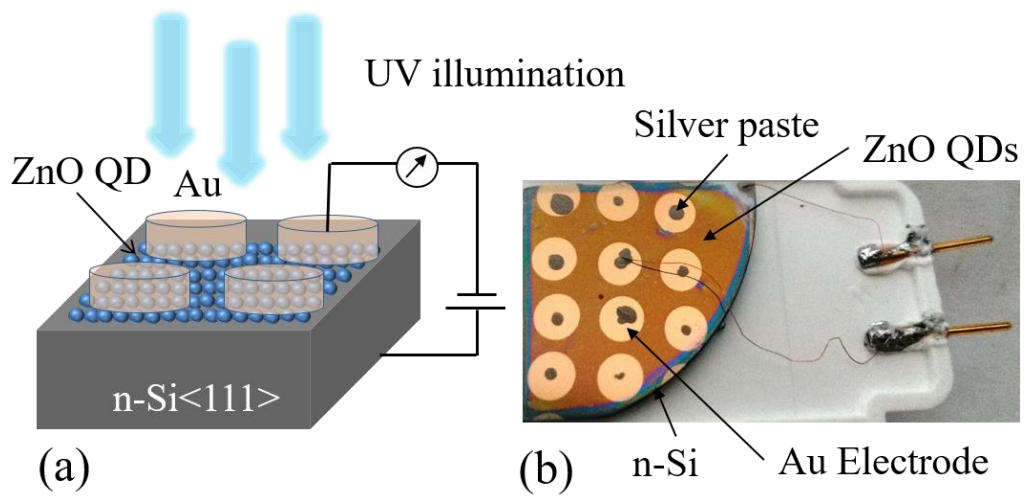


**Figure 2.4:** (a) Device Structure of Au/ZnO QDs Schottky photodiode (b) Fabricated device on n-Si and packaged using silver paste.

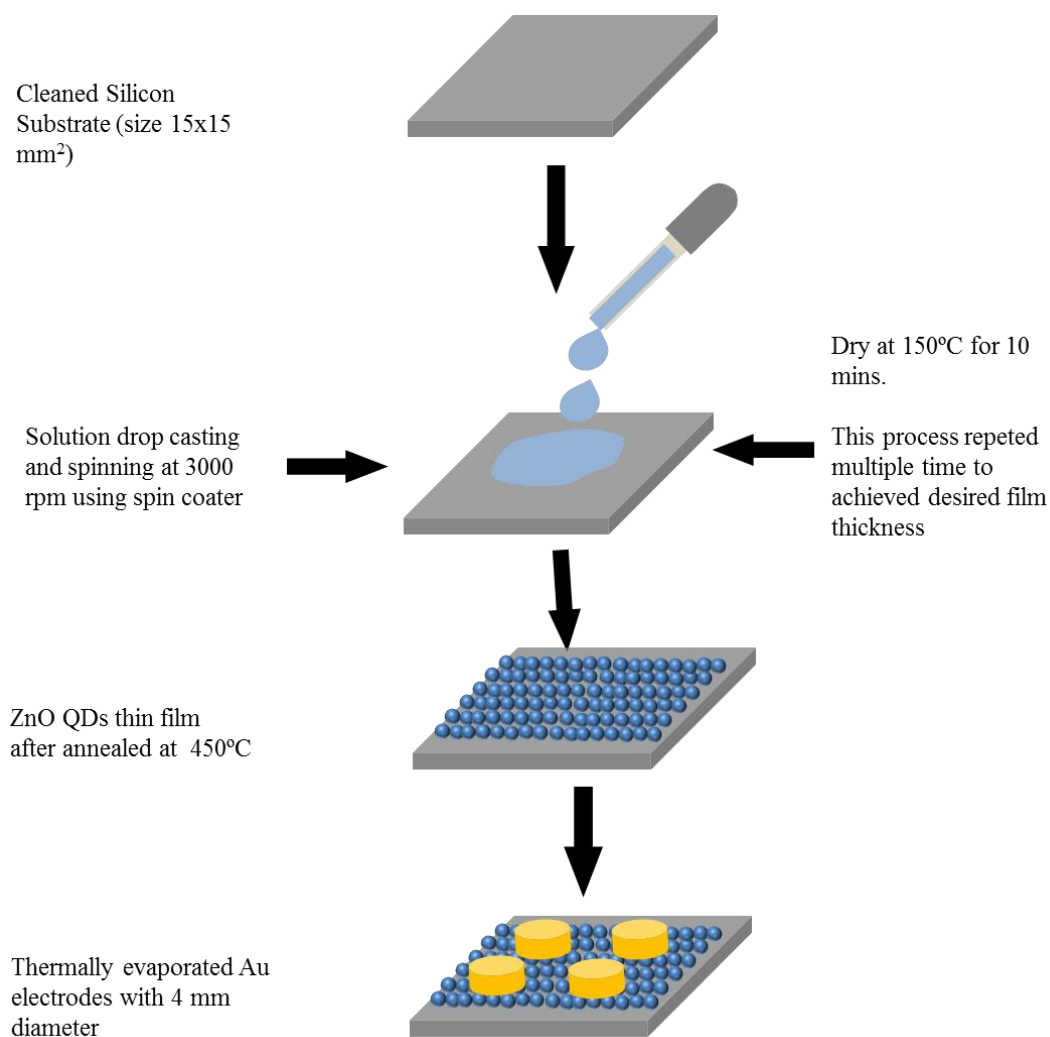


**Figure 2. 5:** Fabrication flow of process

## 2.3 Result and Discussion

### 2.3.1 Structural Characterization of as-grown ZnO QD

The surface morphology of as-grown ZnO QDs is analyzed using TEM (TECHNAI G2 20 TWIN) image shown in Figure 2. 6 (a). The measured particle size of  $\sim 2.53$  nm of the ZnO QDs is smaller than the grain size obtained by Guo et al. (D.-Y. Guo *et al.*, 2014). Further, the particle size is also smaller than the Bohr's radius (i.e.  $\sim 2.87$ nm of ZnO) thereby confirming the QDs nature of the colloidal ZnO nanoparticles. The diffraction pattern and the concentric rings shown in Figure 2. 6 (b) and Figure 2. 7 (a) confirm the crystalline nature of the as-grown and annealed ZnO QDs at 450 °C. The



TEM image of ZnO QDs annealed at 450°C is shown in Figure 2. 7 (b). It shows that the particle size increases with the increasing temperature of annealing.

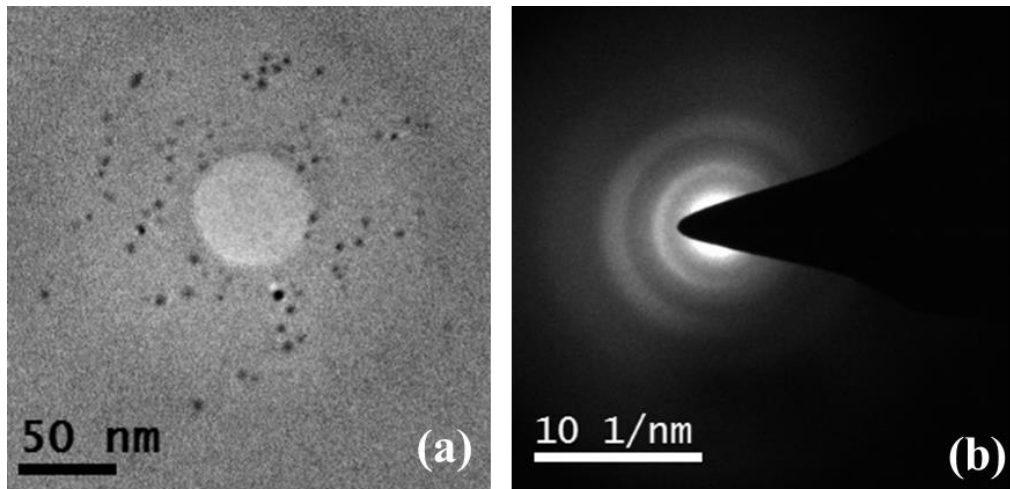


**Figure 2. 6:** (a) TEM image of as-grown ZnO QDs with a particle size of ~2.53 nm, and (b) Diffraction pattern of as grown ZnO QDs

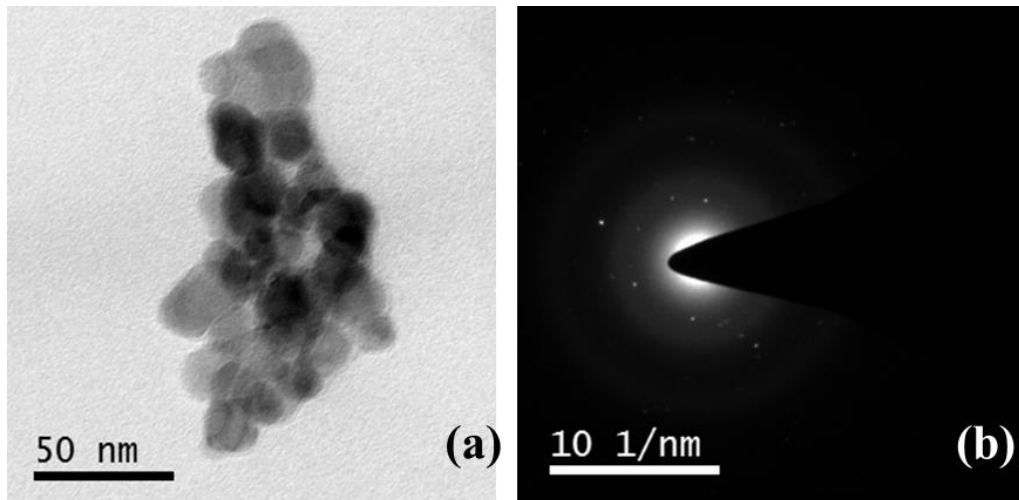


**Figure 2. 7:** (a) TEM image of ZnO QDs annealed at 450°C with a particle size of ~13.80 nm (b) Diffraction pattern of ZnO QD annealed at 450°C

**X-ray diffraction (XRD):** The crystalline structure of the as-grown ZnO QDs as shown in Figure 2. 8 also determined by analyzing the XRD diffraction pattern (model no. XDMAX, PC-20, 18 kW Cu rotating anode, Rigaku, Tokyo, Japan) in continuous scan mode from  $2\theta = 30^\circ$ - $60^\circ$  with a slow scanning speed.

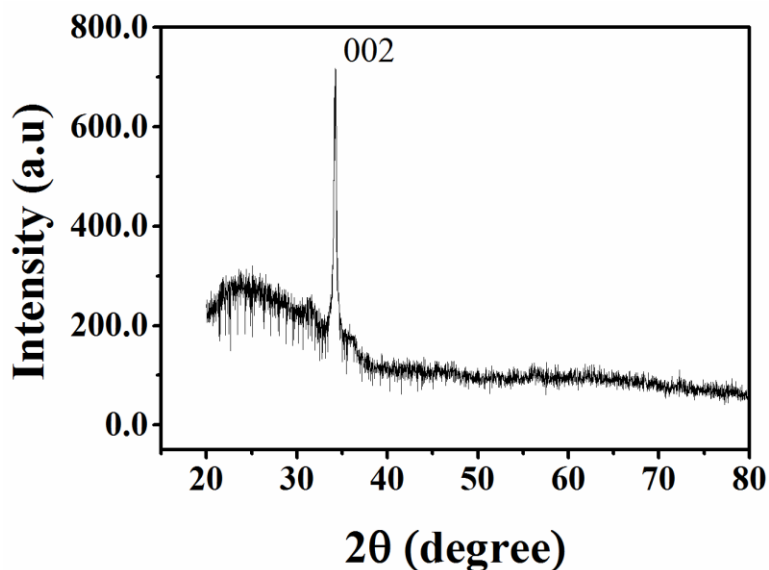


Figure 2. 8: XRD pattern of ZnO QDs annealed at 450 °C

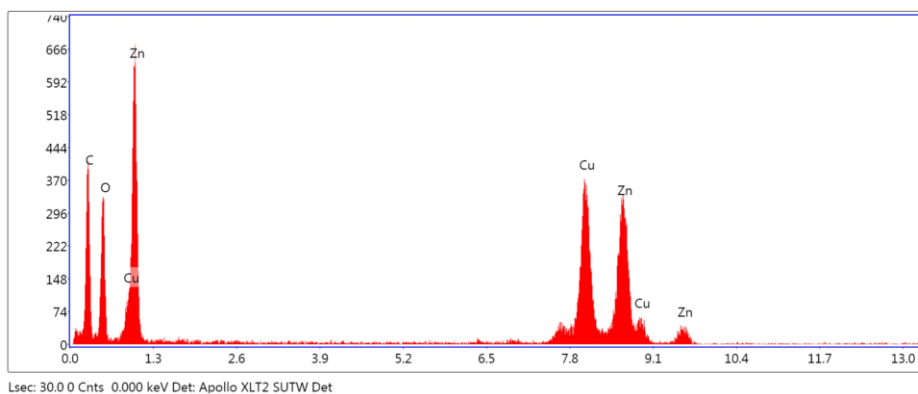
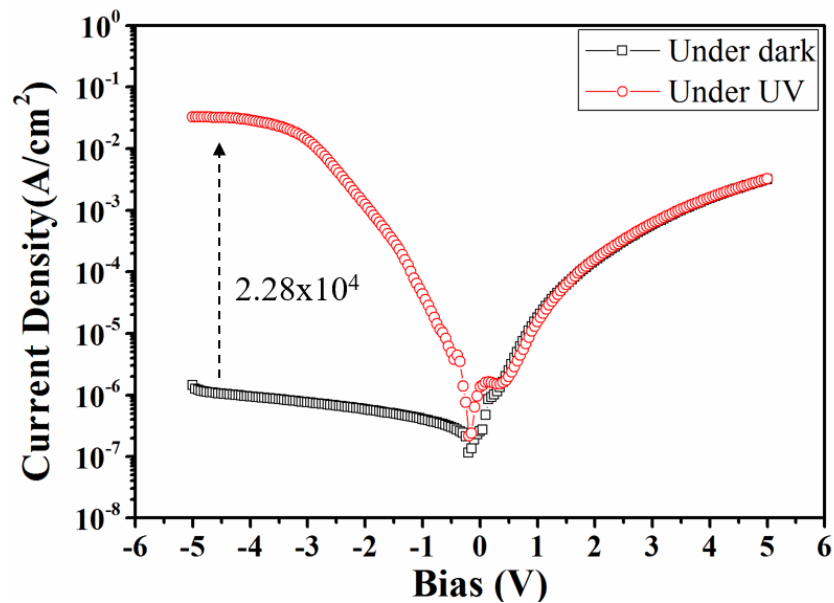


Figure 2. 9: EDS spectra of the as-grown ZnO QDs on carbon copper grid

**Energy dispersive spectrum (EDS) of the ZnO QDs:** The chemical composition of ZnO QDs thin films grown on the carbon copper grid have been determined by the energy dispersive spectrum (EDS) as shown in Figure 2. 9. A good amount of atomic percentages of zinc and oxygen atoms has been found in the EDS spectrum. The peak of the Cu and carbon material is also present in the EDS spectrum due to the copper grid. No peak of any other materials or impurities is observed in the EDS spectrum. This clearly shows that no catalyst metal is involved in the growth of the ZnO QDs.

### 2.3.2 Electro-Optical Characterization

This section describe the electrical characteristics of the Schottky photodiode from the applied bias -5 to 5 V under the dark and UV illumination and also characterize the Schottky diode in terms of the C-V. The electro-optical characteristics such as responsivity versus wavelengths and time response are measured under the dark and UV illumination in this section.



**Figure 2. 10:** J-V characteristics of Au/ZnO Schottky photodiode under dark and UV illumination at 365 nm from the UV LED light with  $800 \mu\text{W}/\text{cm}^2$  optical power.

#### 2.3.2.1 Current Voltage Characterization

The current density against voltage (J-V) characteristics of Au/ZnO Schottky photodiode are shown in Figure 2. 10 measured using semiconductor parameter analyzer (B1500A, KeySight as shown in Figure 2. 11). The J-V characteristics are measured under dark and illumination of single UV LED ( $800 \mu\text{W}/\text{cm}^2$  at 365 nm). The J-V characteristics clearly show the rectifying behavior with the rectification ratio as high as  $2.21 \times 10^3$  in the dark condition. The photocurrent to dark current ratio which is known as ‘contrast ratio’ is also calculated under the illumination of UV LED at an

applied bias of -5 V. The Au/ZnO Schottky photodiode shows very high contrast ratio of  $2.289 \times 10^4$  that indicates a large amount of photo carrier generation under the illumination of UV LED. A high value of photocurrent were attributed due to the large surface to volume ratio of the ZnO QDs and the potential barrier between the two adjacent quantum dots (Xu *et al.*, 2014).

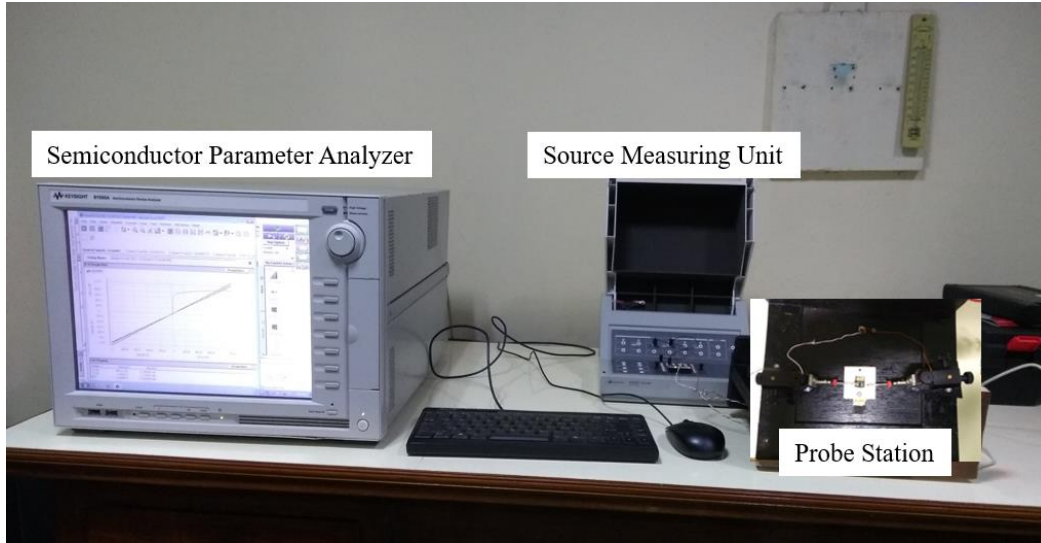


**Figure 2. 11:** Experimental measurement setup for electrical characterization

The Forward current, Barrier height and the ideality factor were extracted from the equation (2.1), (2.2) and (2.3) respectively (Yadav *et al.*, 2015) under the dark condition at room temperature.

$$I = I_0 \left\{ AA^* T^2 \exp\left(-\frac{q\phi_{B,eff}}{kT}\right) \right\} \exp\left(\frac{qV}{nkT}\right) \quad (2.1)$$

$$\phi_{B,eff} = -\frac{kT}{q} \ln\left(\frac{I_0}{AA^* T^2}\right) \quad (2.2)$$

$$n = \frac{q}{kT} \frac{dV}{d \ln(I)} \quad (2.3)$$

where  $A$  is the contact area ( $0.1256 \text{ cm}^2$ ),  $q$  is an electronic charge,  $V$  is applied bias,  $I_0$  is the reverse saturation current,  $T$  is temperature,  $k$  is the Boltzmann constant, and  $A^*$  is the Richardson constant. Following the standard methodologies described in the literature (Aydoğan *et al.*, 2009), (Werner and Güttler, 1991), the values of the reverse saturation current ( $I_0$ ), barrier height ( $\phi_{B,eff}$ ) and ideality factor ( $n$ ) are estimated as 15 nA, 0.80 eV and 2.57 from Eqs. (2.1), (2.2) and (2.3) respectively. It is important to note that the estimated value (i.e. 2.57) of the ideality factor is much larger than its ideal value of unity (i.e.  $n=1$ ). In general, for a spatially homogeneous (i.e. more or less atomically flat) interface between the metal and semiconductor of a Schottky junction, the ideality factor  $n > 1$  is attributed to several effects such as the interface states at the Au/ZnO interface, image force barrier lowering due to the electric field at the interface, and generation/recombination currents within the space-charge region (Werner and Güttler, 1991). However, for any practical Schottky junction without any interfacial layer between the metal and semiconductor, the deviation of the ideality factor from the ideal value of unity is resulted from the spatial inhomogeneities existing at the metal/semiconductor interface (Werner and Güttler, 1991). Thus, the ideality factor of  $n=2.57 (>1)$  observed in the present study for the Au/ZnO QDs Schottky diode may be attributed to the well-known barrier inhomogeneity phenomenon existing in any practical Schottky junction (Werner and Güttler, 1991).

### 2.3.2.2 Capacitance Voltage characteristics

The measured C-V and  $(A^2/C^2) - V$  characteristics as shown in Figure 2. 12 of the Schottky photodiode following the standard methodology described by Somvanshi and Jit (Somvanshi and Jit, 2014), the built-in potential ( $V_{bi}$ ) for the Au/ZnO QDs, the carrier concentration ( $N_D$ ) of the ZnO QDs layer and barrier height for the Au/ZnO QDs

Schottky contact have been estimated as  $\sim 0.75$  V,  $\sim 9.495 \times 10^{16} \text{ cm}^{-3}$ , 0.86 eV respectively. Note that the difference of about 0.06 eV between the barrier heights measured from the I-V and C-V characteristics is attributed to the barrier inhomogeneity phenomenon at the Schottky junction interface (Werner and Güttler, 1991; Aydođan et al., 2009; Brillson and Lu, 2011).

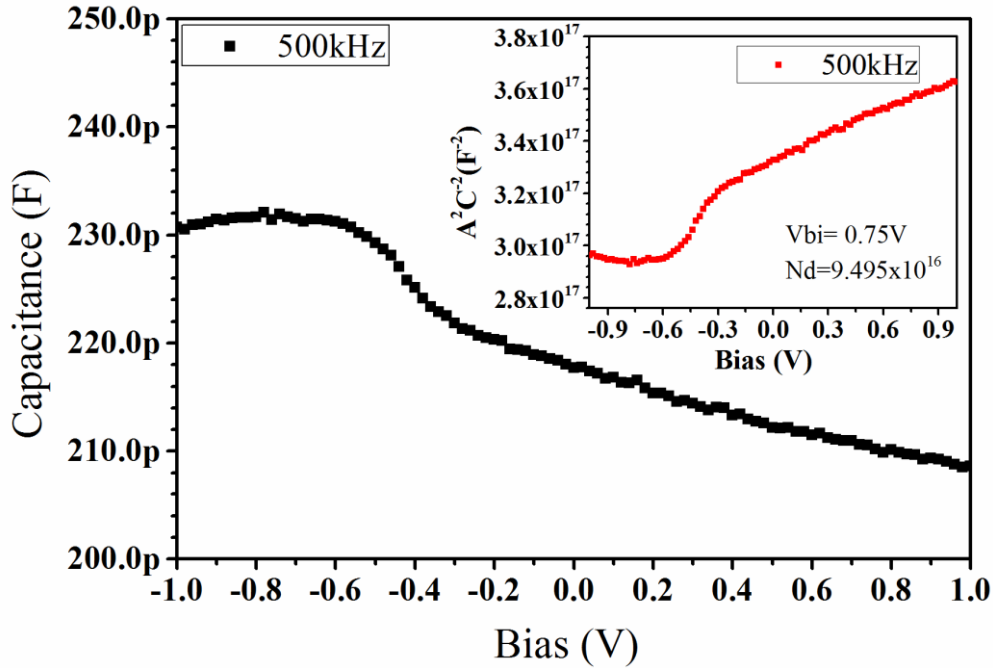


**Figure 2. 12:** C-V characteristic of the Au/ZnO Quantum Dot Schottky photodiode at 500 kHz.

### 2.3.2.3 Responsivity Characterization

The photodetector Responsivity ( $R$ ) is the figure of merit determined using Eq. 1.10 as discussed in chapter 1, measured at an applied bias of -5 volts under the illumination of wavelength 365 nm with an optical power density of  $800 \mu\text{W}/\text{cm}^2$ .

The detectivity of the photodiode can be determined by calculating the  $RA$  product, where  $RA$  is a resistance area product at an applied bias.

$$RA = \left( \frac{\partial J}{\partial V} \right)^{-1} = \frac{kT}{qJ} \quad (2.4)$$

$$D = \frac{\lambda \eta q}{hc} \left( \frac{RA}{4kT} \right)^{1/2} = 1.57 \times 10^{14} \text{ cmHz}^{1/2} \text{ W}^{-1} \quad (2.5)$$

The ZnO QDs based Schottky photodiodes shows the maximum responsivity reported till date in the literature (41.17 (this work) > 8.39 A/W (Yadav et al., 2015)). This huge improvement in the responsivity clearly indicates a certain amount of other active factors, which is participating in the photo-response including with oxygen chemisorption (Xu *et al.*, 2014). In the case of ZnO QDs, the surface energy of QDs is very high, and oxygen molecule can easily adsorb on the surface of the QDs and get ionized by capturing the free electron under the dark condition (Jin *et al.*, 2008; Xu *et al.*, 2014; Yadav *et al.*, 2015; Yu and Tian, 2016). This depletion of charge carriers from the surface of QDs creates the low conductive depletion region between two adjacent QDs as shown in Figure 2. 13 (a) (Xu *et al.*, 2014). Thus, the introduction of depletion region add the surface potential barrier between the two adjacent QDs and bends the energy band upward. Such kind of ZnO thin film is the assembly of the closely packed ZnO QDs in which the junction barrier forms along the QDs, is analogues to the back to back Schottky barriers (Xu *et al.*, 2014). Particularly, in the case of small size ZnO QDs, the number of interfaces for a given thickness is very large, and this interfacial behaviour is a very dominating factor of carrier transport properties (Ma and Su, 2011). Under the illumination of UV, the ZnO QDs absorb the incident photons according to their forbidden energy band. This absorption of photons creates the electron-hole pair on the surface of the quantum dots as shown in Figure 2. 13 (b). The photogenerated holes migrates to the surface and liberates the adsorbed oxygen from the surface of the ZnO QDs. This liberation of oxygen reduces the surface potential barrier height also shown in Figure 2. 13 (b) and leading to the sharp increase

in the photogenerated current as also shown in Figure 2. 10 J-V characteristics of the device under the illumination of UV LED source.

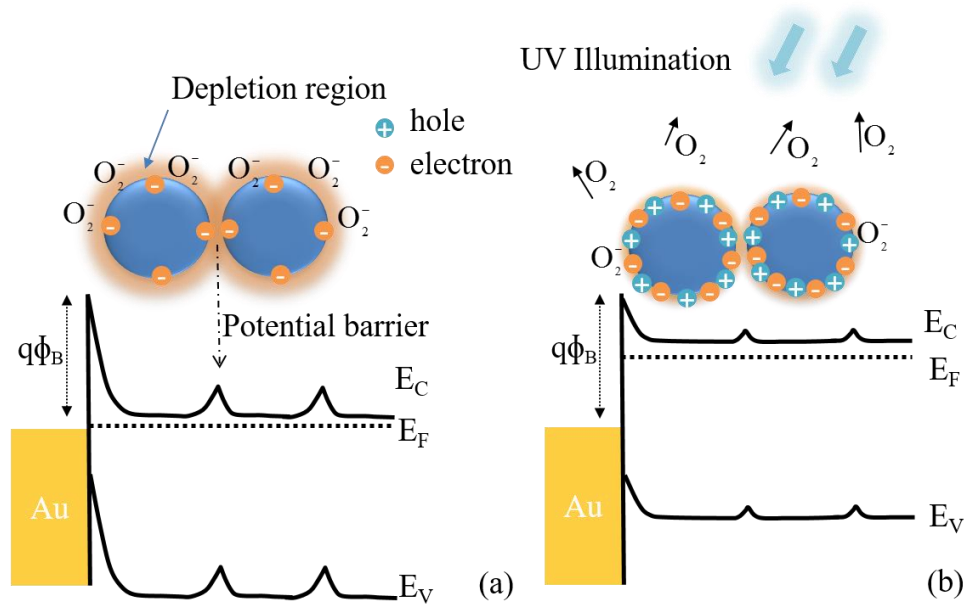


**Figure 2. 13:** Charge distribution and energy band on the surface of the ZnO QDs under the UV illumination and dark

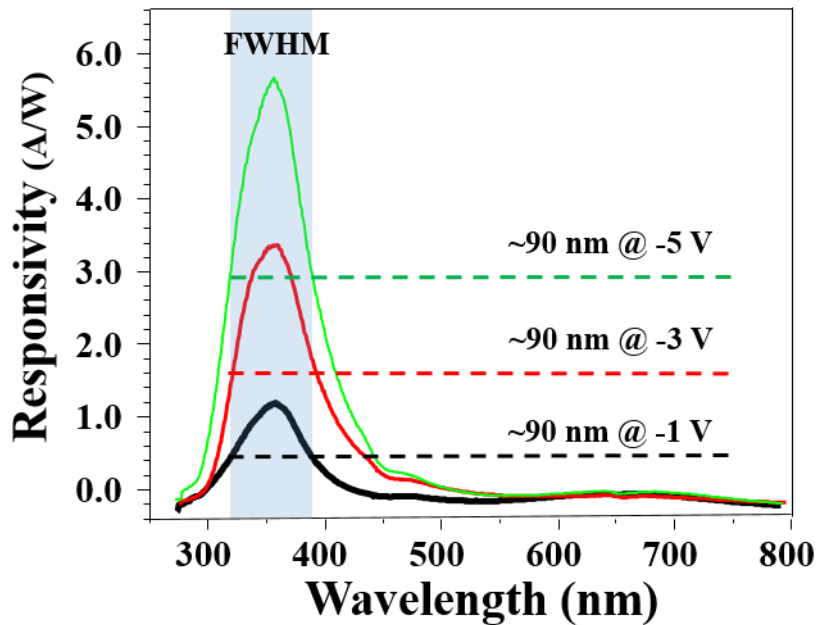


**Figure 2. 14:** Responsivity spectrum of the Au/ZnO QDs Schottky photodiode at an applied -5 V, -3 V, and -1 V bias.



The responsivity spectrum of the Schottky photodiode is measured against the wavelength from 250 nm to 900 nm shown in Figure 2. 14. The spectral response of the Schottky photodiode is measured by using monochromator (Princeton Instruments, SP2150i) and digital multimeter (Agilent, 34410A) at a scan rate of 60 nm/min, the experimental setup for measurement of the responsivity shown in Figure 2. 15. The optical power density of the light sources (monochromatic and UV LED) are measured using PM100D, Thorlabs detector. The responsivity curve of the Schottky photodiode is analyzed for the applied bias of -5 V, -3 V and -1 V. The responsivity spectrum of the Schottky photodiode shows consistent selective response with an FWHM of ~90 nm (300 to 390 nm) which lies completely in the UV region. The peak responsivity of 6.01 A/W was measured at 365 nm wavelength for an applied bias of -5 V for a very low optical power density of 83  $\mu\text{W}/\text{cm}^2$ . The spectrum selective absorption nature of the Schottky photodiode is attributed due to two reasons:

1. The ZnO QDs with a very small particle size ( $<$  Bohr's radius  $\sim 2.87$  nm) exhibits very high quantum confinement, with an increase of particle size there is a decrement in quantum confinement. The QDs possess discrete energy states, and the separation of the quantized states are dependent on the confinement of QDs, higher the quantum confinement higher is the separation. The ZnO QDs annealed at 450  $^{\circ}\text{C}$  shows a quantum confinement which is higher than the bulk ZnO leading to the spectrum selective response of the photodiode.
2. The thin film of Au electrode are also responsible for the narrow spectrum of the photodiode. Figure 2. 16 shows the transmittance spectrum of the Au thin film and absorbance characteristics of the ZnO QDs over the quartz

substrate that are measured using Reflectometer (F-20 thin film analyzer, Filmetrics). This result clearly indicates that the Au thin film exhibits ~0% transmittance below 300 nm, while it shows sharp rise at 350 nm to ~45%. This combination of Au thin film with ZnO QDs thin film absorbs the photons with a wavelength shorter than 390 nm and greater than 300 nm.

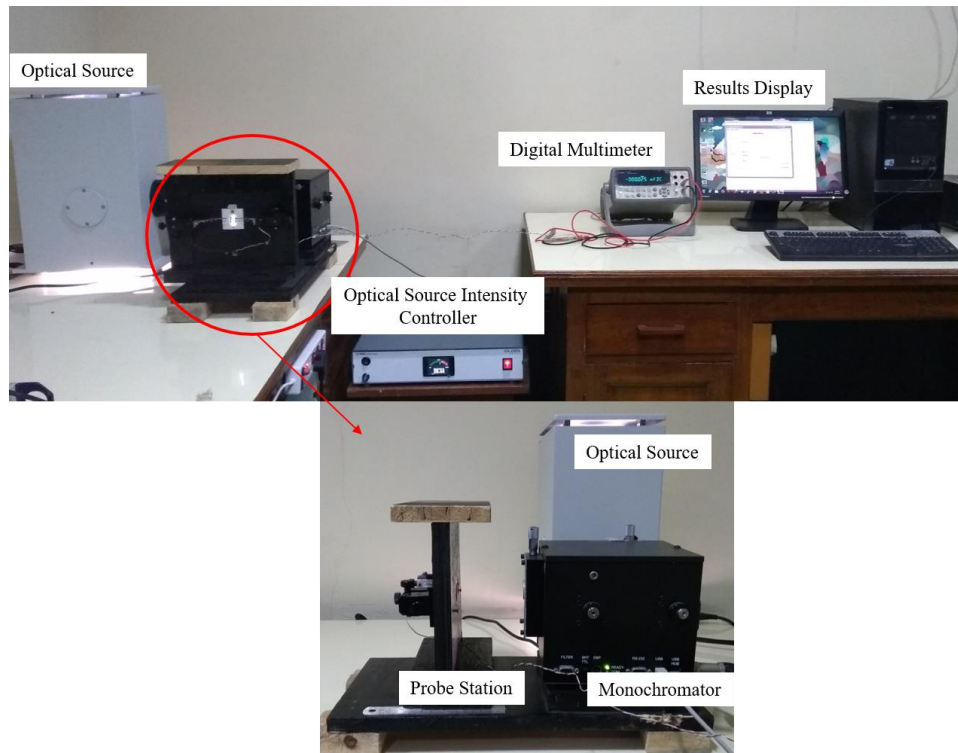


**Figure 2. 15:** Experimental measurement setup for the photocurrent vs wavelengths measurement.

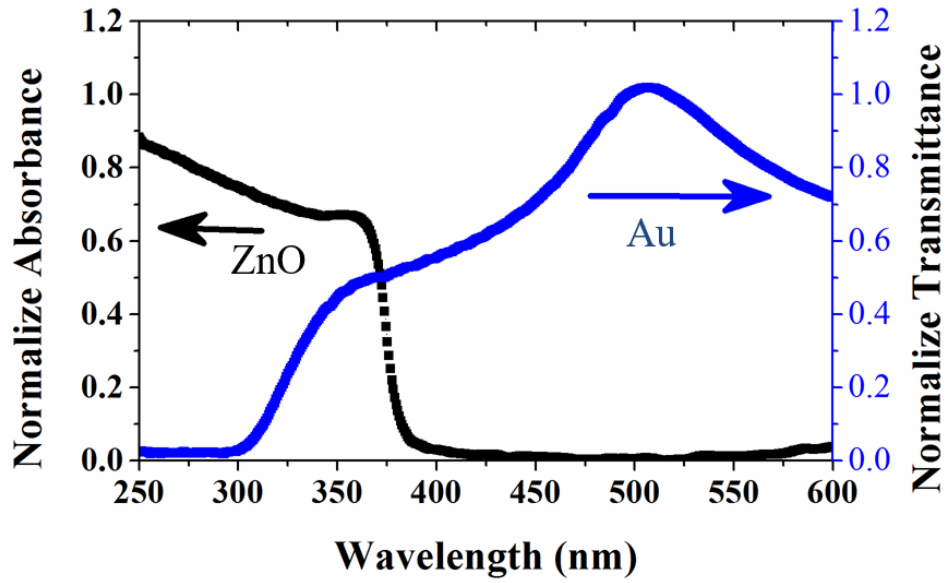


**Figure 2.16:** Normalized Absorption of ZnO Quantum Dots thin film (thickness  $\sim 200\text{nm}$ ) and Transmittance of Au thin film (thickness  $\sim 70\text{nm}$ ).

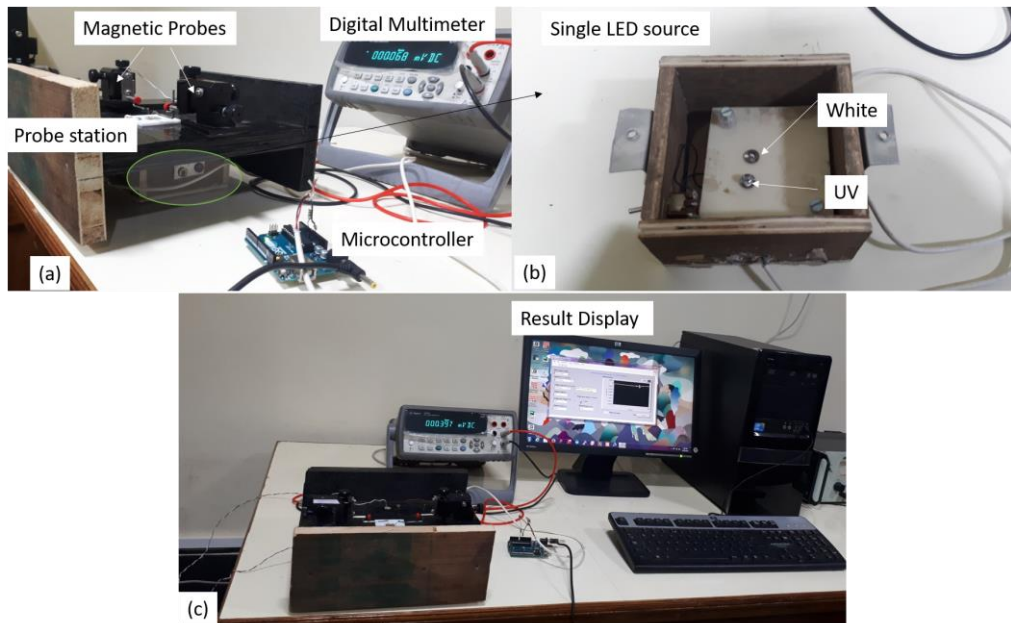


**Figure 2.17:** Experimental setup for the time response measurement (a) UV LED source provides the UV pulses (c) complete time response measurement setup with data acquisition using LabView.

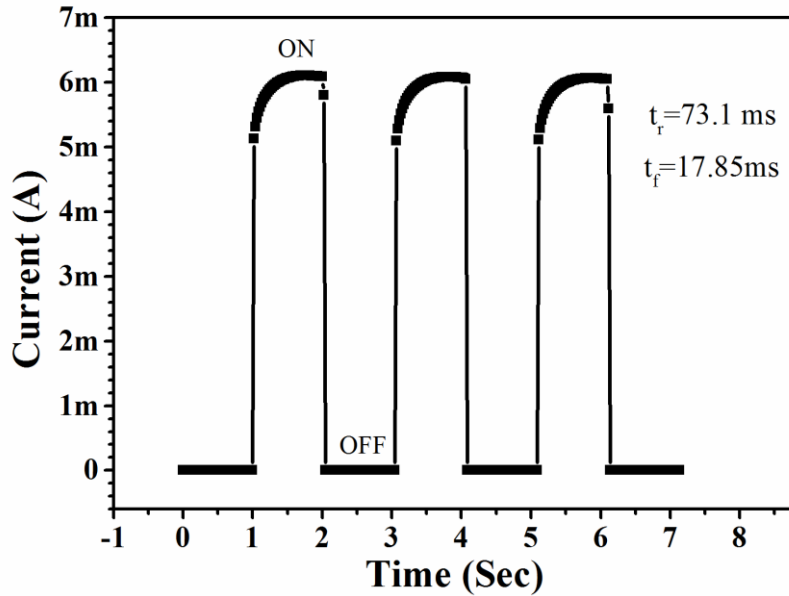


**Figure 2. 18:** Time response of the Au/ZnO QDs Schottky photodiode under the illumination of UV LED pulsating 1sec ON and OFF.

#### 2.3.2.4 Time response analysis

The transient analysis of the Schottky photodiode was measured at -5 V bias under the illumination of the light source with array of 2 x 2 UV LEDs with the central wavelength around ~390 nm. We have measured output power density (by Thorlabs PM100D power meter) at wavelength 365 nm from our LED source driven by the Arduino® Microcontroller with ON and OFF periods of 1 sec duration. The experimental setup for the measurement of time response is shown in Figure 2. 17. The Schottky photodiode shows the fast response with a rise time of 73.1 ms (10-90%) and recovery time of 17.85 ms (90-10%) as shown in Figure 2. 18. The fast time response characteristics of the ZnO QDs based Schottky photodiode is due to the back to back barrier between adjacent QDs. This barrier improves the switching capabilities of the Schottky photodiode. The various performance parameters of the Schottky photodiode studied in this article are summarized and compared with other reported works in the literature are shown in table 2.1.

**Table 2.1.** Comparison of the electrical and optical parameters of our photodiode with reported devices in the articles

Figure of merits	This work	(Yu and Tian, 2016)	(Xu <i>et al.</i> , 2014)	(Kumar <i>et al.</i> , 2017)	(Yadav <i>et al.</i> , 2015)	(Rajan <i>et al.</i> , 2016)
Device structure	Au/ ZnO Schottky Diode	Au/ZnO MSM	Au/ZnO MSM	Ag/ ZnO MSM	Pd/ZnO Schottky Diode	Au/ZnO Schottky Diode
Applied Bias (V)	-5	3	5	2	-5	-5
Responsivity (A/W)	41.17	0.052	504	15.04	8.39	-
Detectivity (cmHz <sup>1/2</sup> W <sup>-1</sup> )	1.57x10 <sup>14</sup>	6.2x10 <sup>6</sup>	-	1.97 x10 <sup>14</sup>	7.5x10 <sup>12</sup>	-
Illuminated optical power (W/cm <sup>2</sup> )	800μ	-	22.9m	-	650μ	-
Contrast ratio	2.28x10 <sup>4</sup>	-	-	-	5.33x10 <sup>3</sup>	-
Ideality factor	2.57	-	-	-	1.50	6
Barrier height (eV)	0.80	-	-	-	0.75	0.804
Rectification ratio	2.21x10 <sup>3</sup>	-	-	-	-	93
Deposition Technique	Solution processed	RF sputtering	Solution processed	Solution processed	Solution processed	RF sputtering

## 2.4 Conclusion

In this chapter, we have demonstrated the fabrication of highly sensitive and spectrum selective Au/ZnO quantum dot Schottky photodiode. The photodiode has highest responsivity and contrast ratio of 41.17 A/W and 2.289 x 10<sup>4</sup> respectively under the UV illumination ( $\lambda=365$  nm) of 800μW/cm<sup>2</sup> optical power density. The transmittance of Au thin film and absorbance of the ZnO QDs opens a narrow window for the spectrum selective response in the UV region with FWHM of ~90 nm, which is

clearly indicating the total blindness of the photodetector in the visible region. This photodiode also exhibits the fast response (73.1 ms) and quick full recovery (17.85 ms) at an applied bias -5 V, which shows the fast reliable detection properties of the photodiode under repeated illumination of UV light.